Turkish Journal of Electrical Engineering & Computer Sciences

http://journals.tubitak.gov.tr/elektrik/

Research Article

Turk J Elec Eng & Comp Sci
(2015) 23: 187 – 200

doi:10.3906/elk-1208-50

MRAS-based sensorless speed backstepping control for induction machine, using a flux sliding mode observer

Mohamed MOUTCHOU*, **Ahmed ABBOU, Hassan MAHMOUDI**
Mohammadia School of Engineering, Mohamed V University, Rabat, Morocco

Received: 14.08.2012 • **Accepted:** 28.03.2013 • **Published Online:** 12.01.2015 • **Printed:** 09.02.2015

Abstract: In this paper, an induction machine rotor speed and rotor flux control using a sensorless backstepping control scheme is discussed. The most interesting point of this technique is that it deals with the nonlinearity of a high-order system by using the virtual control variable to make this system simple, and thus the control outputs can be derived step by step through appropriate Lyapunov functions. To avoid the use of a mechanical sensor, the rotor speed estimation is made by an observer using the model reference adaptive system (MRAS) technique; in order to estimate rotor flux, a sliding mode observer is proposed in this work. Simulation results are presented to validate and prove the effectiveness of the proposed sensorless control.

Key words: Backstepping control, MRAS observer, sliding mode, Lyapunov stability, induction motor drive

1. Introduction

The induction machine, by its construction, is the most robust and cheapest machine on the market. Advances in control and significant technological advances in the fields of power electronics and microelectronics have made possible the implementation of efficient controls for this machine, making it a formidable competitor in the areas of variable speed and torque control.

However, many problems remain due to its complex and nonlinear mathematical model, which involves parameters that vary with temperature, frequency, and other operating conditions. The variability of the parameters has significant effects on the accuracy of control speed and torque, as well as other operating performance measures of the motor.

Those difficulties have whetted the curiosity of scientists and researchers in laboratories, as evidenced by the growing number of publications that discuss the subject. Different control strategies have been developed, like field-oriented control, proposed by Blaschke [1]; this control technique has led to a radical change in control of the asynchronous machine, thanks to the quality of dynamic performance that it brings. In vector control, the torque and flux are decoupled by a suitable decoupling network. The flux component and the torque are then controlled independently by stator direct-axis current and stator quadratic-axis current respectively to control the induction motor (IM) as a separately excited DC motor [2,3]. The high performance of such a strategy may deteriorate in practice due to plant uncertainties.

Others techniques have been conceived, like the linearization input–output technique [4–6]. The technique of linearization input–output based on differential geometry allows diffeomorphic transformation and state

*Correspondence: m.moutchou@yahoo.fr

feedback. This method cancels the nonlinear terms in the plant model, which fails when the physical parameters vary.

By contrast, passivity-based control [7,8] does not cancel out all the nonlinearity, but does ensure system stability by adding a damping term to the total energy of the system. It is characterized by its robustness with regard to parameter uncertainties, but its experimental implementation is still difficult.

The sliding mode control is characterized by simplicity of design and attractive robustness properties. Its major drawback is the chattering phenomenon [9–12].

The backstepping control approach is more recent. Its present form is due to the work of Freeman and Kokotovic, Krstic et al., and Ikhouane and Krstic [13–15]. Based on the Lyapunov stability tools, this approach offers great flexibility in the synthesis of the regulator and naturally lends itself to an adaptive extension to the case [16–21]. This control technique offers good performance in both steady state and transient operations, even in the presence of parameter variations and load torque disturbances.

These control techniques cannot guarantee good performance without the use of a suitable state observer. Among the observation techniques used are the sliding mode techniques used in this work to estimate flux, and the model reference adaptive system (MRAS) technique, which was used in sensorless IM drives for the first time by Schauder (22). The MRAS technique is interesting since it leads to a relatively easy-to-implement system with high-speed adaptation [22–25].

In this work, we chose to use a backstepping control technique based on the induction machine model represented in the fixed stator frame, (α, β). This control technique is suitable for a nonlinear system (e.g., IM). In order to obtain better performance, we designed 2 observers, the first for speed estimation based on the MRAS technique and the second for flux component estimation using sliding mode theories. Simulation results, given at the end, illustrate the good performance of this control method. The structure of this control is presented in Figure 1.

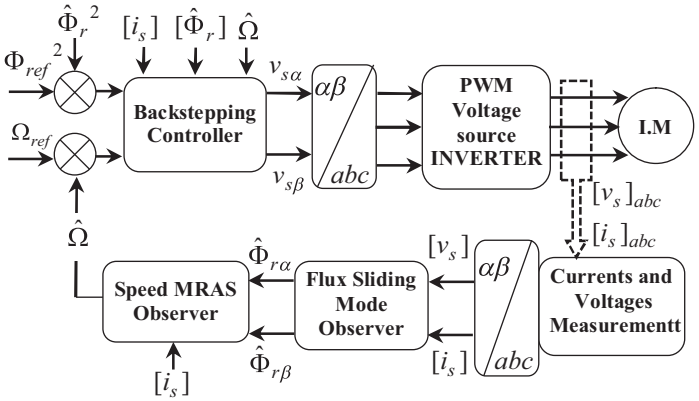

Figure 1. Control structure.

2. Model description of the induction machine

In order to reduce the complexity of the 3-phase model, an equivalent 2-phase representation was chosen. Under the assumptions of linearity of the magnetic circuit and neglecting iron losses, a 2-phase IM model can

be described in the fixed stator reference frame (α , β) as below:

$$\begin{cases} \frac{di_{s\alpha}}{dt} = -\gamma.i_{s\alpha} + k.\lambda_r.\Phi_{r\alpha} + k.p.\Omega.\Phi_{r\beta} + \delta.v_{s\alpha} \\ \frac{di_{s\beta}}{dt} = -\gamma.i_{s\beta} - k.p.\Omega.\Phi_{r\alpha} + k.\lambda_r.\Phi_{r\beta} + \delta.v_{s\beta} \\ \frac{d\Phi_{r\alpha}}{dt} = \lambda_r.(L_m.i_{s\alpha} - \Phi_{r\alpha}) - p.\Omega.\Phi_{r\beta} \\ \frac{d\Phi_{r\beta}}{dt} = \lambda_r.(L_m.i_{s\beta} - \Phi_{r\beta}) + p.\Omega.\Phi_{r\alpha} \\ \frac{d\Omega}{dt} = \frac{\mu}{J}.(\Phi_{r\alpha}.i_{s\beta} - \Phi_{r\beta}.i_{s\alpha}) - \frac{f}{J}.\Omega - \frac{T_L}{J} \end{cases} \quad (1)$$

where:

$$\sigma = 1 - \frac{L_m^2}{L_r.L_s} \;\; ; \;\; k = \frac{L_m}{\sigma L_s L_r}; \;\; T_r = \frac{L_r}{R_r} \;\; ; \;\; \lambda_r = \frac{R_r}{L_r}; \;\; \gamma = \frac{1}{\sigma L_s}\left(R_s + \frac{R_r.L_m^2}{L_r^2}\right) \;\; ; \;\; \mu = p\frac{L_m}{L_r} \;\; ; \;\; \delta = \frac{1}{\sigma.L_s}.$$

3. Induction machine backstepping control

We saw that the dynamic equations of the induction machine are nonlinear, which makes the control difficult to achieve. However, by using backstepping techniques, we can control the system by treating it progressively piece by piece from the outputs, backstepping over "virtual controls" to real controls (stator voltages).

The backstepping control design is based on the use of the so-called "virtual control" to systematically deconstruct a complex nonlinear control design problem into simpler, smaller ones, by dividing the backstepping design into various design steps. In each step, we deal with an easier, single-input/single-output design problem, and each step provides a reference for the next design step.

This approach is different from conventional feedback linearization in that it can avoid cancellation of useful nonlinearities in aiming to achieve the objectives of stabilization and tracking.

The asymptotic stability of the resulting closed-loop system is guaranteed according to Lyapunov's stability theorem.

3.1. First step

In the first, we search for the virtual control that ensures the asymptotic convergence of both the flux-tracking error and the speed-tracking error to zero.

The rotor speed and rotor flux module tracking error are defined by:

$$\begin{cases} e_1 = \Omega_{ref} - \Omega \\ z_1 = \Phi_{ref}^2 - \Phi_r^2 \end{cases} \quad (2)$$

where Ω_{ref} and Φ_{ref}^2 are respectively the reference of speed and rotor flux modulus.

$$\Phi_r^2 = \Phi_{r\alpha}^2 + \Phi_{r\beta}^2.$$

Then the error dynamic equations are:

$$\begin{cases} \dot{e}_1 = \dot{\Omega}_{ref} - \left(\frac{\mu}{J}.(\Phi_{r\alpha}.i_{s\beta} - \Phi_{r\beta}.i_{s\alpha}) - \frac{f}{J}.\Omega - \frac{T_L}{J}\right) \\ \dot{z}_1 = \frac{d}{dt}\left(\Phi_{ref}^2\right) - 2.\lambda_r.L_m.(\Phi_{r\alpha}.i_{s\alpha} + \Phi_{r\beta}.i_{s\beta}) + 2.\lambda_r.\Phi_r^2 \end{cases} \quad (3)$$

By putting the virtual control expressions below,

$$\begin{cases} \alpha_1 = (\Phi_{r\alpha}.i_{s\beta} - \Phi_{r\beta}.i_{s\alpha}) \\ \beta_1 = (\Phi_{r\alpha}.i_{s\alpha} + \Phi_{r\beta}.i_{s\beta}) \end{cases} \tag{4}$$

we can write Eq. (3) in the following form:

$$\begin{cases} \dot{e}_1 = \dot{\Omega}_{ref} - \frac{\mu}{J}.\alpha_1 + \frac{f}{J}.\Omega + \frac{T_L}{J} \\ \dot{z}_1 = \frac{d}{dt}\left(\Phi_{ref}^2\right) - 2.\lambda_r.L_m..\beta_1 + 2.\lambda_r.\Phi_r^2 \end{cases} \tag{5}$$

Let us check the tracking error stability by choosing the Lyapunov candidate function (LCF) below:

$$v_1 = \frac{1}{2}.e_1^2 + \frac{1}{2}.e_2^2 \tag{6}$$

The derivative of Eq. (6) gives: $\dot{v}_1 = e_1.\dot{e}_1 + e_2.\dot{e}_2$.

Let us consider the following virtual control reference that stabilizes the tracking errors e_1 and z_1:

$$\begin{cases} \alpha_{1ref} = \frac{J}{\mu}.\left(c_1.e_1 + \dot{\Omega}_{ref} + \frac{f}{J}.\Omega + \frac{T_L}{J}\right) \\ \beta_{1ref} = \frac{1}{2.\lambda_r.L_m}\left(d_1.z_1 + \frac{d}{dt}\left(\Phi_{ref}^2\right) + 2.\lambda_r.\Phi_r^2\right) \end{cases} \tag{7}$$

where $c_1 > 0$ and $d_1 > 0$ are the positive design gains that determine the dynamic of the closed loop.

Using Eqs. (5) and (7), we get:

$$\begin{cases} \dot{e}_1 = -c_1.e_1 \\ \dot{z}_1 = -d_1.z_1 \end{cases}.$$

The choice of Eq. (7) will then give us:

$$\dot{v}_1 = -c_1.e_1^2 - d_1.z_1^2 \leq 0.$$

This is evidently seminegative definite, so the tracking errors e_1 and z_1 have been stabilized.

3.2. Second step

Previous references, chosen to ensure a stable dynamic of speed- and flux-tracking error, cannot be imposed on the virtual controls without considering errors between them.

Let us define the following errors:

$$\begin{cases} e_2 = \alpha_{1ref} - \alpha_1 \\ z_2 = \beta_{1ref} - \beta_1 \end{cases} \tag{8}$$

One determines the new dynamics of the errors e_1 and z_1, expressed now in terms of e_2 and z_2, by

$$\begin{cases} \dot{e}_1 = -c_1.e_1 + \frac{\mu}{J}.e_2 \\ \dot{z}_1 = -d_1.z_1 + 2.L_m.\lambda_r.z_2 \end{cases} \tag{9}$$

By deriving Eq. (8), we obtain the following error dynamics equations:

$$\begin{cases} \dot{e}_2 = \alpha_2 - \delta.(\Phi_{r\alpha}.v_{s\beta} - \Phi_{r\beta}.v_{s\alpha}) \\ \dot{z}_2 = \beta_2 - \delta.(\Phi_{r\alpha}.v_{s\alpha} + \Phi_{r\beta}.v_{s\beta}) \end{cases} \tag{10}$$

$$\text{where} \begin{cases} \alpha_2 = \dot{\alpha}_{1ref} + (\gamma + \lambda_r).\alpha_1 + \omega.\beta_1 + k\omega.\Phi_r^2 \\ \beta_2 = \dot{\beta}_{1ref} + (\gamma + \lambda_r).\beta_1 - \omega.\alpha_1 - k.\lambda_r.\Phi_r^2 - \lambda_r.L_m.(i_{s\alpha}^2 + i_{s\beta}^2) \\ \omega = p.\Omega \end{cases}.$$

Now that the real control variables $(v_{s\alpha}, v_{s\beta})$ have appeared in Eq. (10), we define the final complete LCF as follows:

$$v_2 = \frac{1}{2}.e_1^2 + \frac{1}{2}.z_1^2 + \frac{1}{2}.e_2^2 + \frac{1}{2}.z_2^2.$$

Thus, the LCF derivative is determined below, by using Eqs. (9) and (10):

$$\begin{aligned} \dot{v}_2 &= -c_1.e_1^2 - d_1.z_1^2 - c_2.e_2^2 - d_2.z_2^2 + e_2.\left(c_2.e_2 + \tfrac{\mu}{J}.e_1 + \alpha_2 - \delta.(\Phi_{r\alpha}.v_{s\beta} - \Phi_{r\beta}.v_{s\alpha})\right) \\ &\quad + z_2.\left(d_2.z_2 + 2.\lambda_r.L_m.z_1 + \beta_2 - \delta.(\Phi_{r\alpha}.v_{s\alpha} + \Phi_{r\beta}.v_{s\beta})\right) \end{aligned},$$

where $c_2 > 0$ and $d_2 > 0$ are the positive design gains that determine the dynamics of the closed loop.

In order to make the LCF derivative be negative definite and have the following expression:

$$\dot{v}_2 = -c_1.e_1^2 - d_1.z_1^2 - c_2.e_2^2 - d_2.z_2^2 \leq 0,$$

we chose voltage control as follows:

$$\Rightarrow \begin{cases} c_2.e_2 + \frac{\mu}{J}.e_1 + \alpha_2 - \delta.\left(\Phi_{r\alpha}.v_{s\beta} - \Phi_{r\beta}.v_{s\alpha}\right) = 0 \\ d_2.z_2 + 2.\lambda_r.L_m.z_1 + \beta_2 - \delta.\left(\Phi_{r\alpha}.v_{s\alpha} + \Phi_{r\beta}.v_{s\beta}\right) = 0 \end{cases},$$

And then we obtain the input controls, $(v_{s\alpha}, v_{s\beta})$:

$$\begin{cases} v_{s\alpha} = \frac{1}{\delta.\Phi_r^2}\left[B.\Phi_{r\alpha} - A.\Phi_{r\beta}\right] \\ v_{s\beta} = \frac{1}{\delta.\Phi_r^2}\left[B.\Phi_{r\beta} + A.\Phi_{r\alpha}\right] \end{cases},$$

$$\text{where} \begin{cases} A = c_2.e_2 + \frac{\mu}{J}.e_1 + \alpha_2 \\ B = d_2.z_2 + 2.\lambda_r.L_m.z_1 + \beta_{\ 2} \end{cases}.$$

4. Rotor flux sliding mode observer (SMO)

Among the control difficulties of the induction machine is that its state is not completely measurable, especially for the rotor flux. Different techniques have been used to estimate these variables in the literature. In this research, we have chosen to use the sliding mode technique because of the benefits it offers in terms of robustness. The flux observer that we are going to design will be used for the backstepping control and for the rotor speed estimation. The structure of the flux observer is shown in Figure 2.

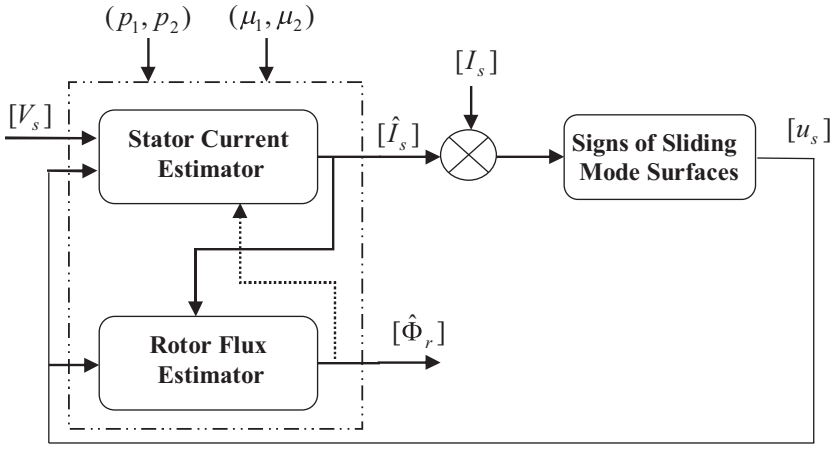

Figure 2. Flux sliding mode observer structure.

4.1. Induction machine model

In this section, we use a model of an asynchronous machine formulated in a stationary stator reference frame, (α, β), as shown below:

$$\begin{cases} \dot{I}_s = -\gamma.I_s + k.A.\Phi_r + \delta.V_s \\ \dot{\Phi}_r = L_m.\lambda_r.I_s - A.\Phi_r \end{cases} \tag{11}$$

with $I_s = [i_{s\alpha} i_{s\beta}]^T$; $\Phi_r = [\Phi_{r\alpha} \Phi_{r\beta}]^T$; $V_s = [v_{s\alpha} v_{s\beta}]^T$; $A = \begin{bmatrix} \lambda_r & \omega \\ -\omega & \lambda_r \end{bmatrix}$.

4.2. Rotor flux SMO model

The equations representing the observer model are given below:

$$\begin{cases} \dot{\hat{I}}_s = -\gamma.\hat{I}_s + k.A.\hat{\Phi}_r + \delta.V_s + D_i.u_s \\ \dot{\hat{\Phi}}_r = L_m.\lambda_r.\hat{I}_s - A.\hat{\Phi}_r + D_\phi.u_s \end{cases} \tag{12}$$

The dynamics of the estimation error are expressed by the following equations:

$$\begin{cases} \dot{\tilde{I}}_s = -\gamma.\tilde{I}_s + k.A.\tilde{\Phi}_r - D_i.u_s \\ \dot{\tilde{\Phi}}_r = L_m.\lambda_r.\tilde{I}_s - A.\tilde{\Phi}_r - D_\phi.u_s \end{cases} \tag{13}$$

where $\tilde{I}_s = I_s - \hat{I}_s$ is the stator current estimation error; $\tilde{\Phi}_r = \Phi_r - \hat{\Phi}_r$ is the rotor flux estimation error; $u_s = [sign(S_1) sign(S_2)]^T$; $S = [s_1 s_2]^T = \eta.(\tilde{I}_s)$ is the sliding mode surface; and D_ϕ, D_i, η are the matrix (2 $\times$ 2) that we will determine later.

4.3. Design of the rotor flux SMO

We consider the following Lyapunov candidate function:

$$V = \frac{1}{2}.S^T.S.$$

Its time derivative is the following:

$$\dot{V} = S^T.\dot{S}.$$

We suppose that $\frac{d\eta}{dt} = 0$; thus, we obtain:

$$\dot{V} = S^T.\eta.\dot{\tilde{I}}_s,$$

$$\dot{V} = S^T.\eta.\left(-\gamma.\tilde{I}_s + k.A.\tilde{\Phi}_r\right) - S^T.\eta.D_i.u_s.$$

In order to have $\dot{V}$ negative definite and satisfy the condition of attractiveness, we must have:

$$S^T.\eta.\left(-\gamma.\tilde{I}_s + k.A.\tilde{\Phi}_r\right) < S^T.\eta.D_i.u_s.$$

If we put

$$\eta.D_i = \begin{bmatrix} \mu_1 & 0 \\ 0 & \mu_2 \end{bmatrix},$$

then we obtain the condition below:

$$\mu_1.|S_1| + \mu_2.|S_2| > S^T.\eta.\left(-\gamma.\tilde{I}_s + k.A.\tilde{\Phi}_r\right).$$

When the sliding mode is reached, the switching surface will verify it:

$$\tilde{I}_s = \dot{\tilde{I}}_s = 0;$$

therefore, we obtain

$$u_s = D_i^{-1}.k.A.\tilde{\Phi}_r.$$

By putting this equation into Eq. (13), we get this equation:

$$\dot{\tilde{\Phi}}_r = -\left(A + D_\phi.D_i^{-1}.k.A\right).\tilde{\Phi}_r.$$

We put: $A + D_\phi.D_i^{-1}.k.A = \mathrm{P}$

$$\Rightarrow \dot{\tilde{\Phi}}_r = -\mathrm{P}.\tilde{\Phi}_r.$$

In order to have exponential convergence, we choose P in the following form:

$$\mathrm{P} = \begin{bmatrix} p_1 & 0 \\ 0 & p_2 \end{bmatrix},$$

where p1 and p2 are positive constants.

Then we obtain the following equation:

$$D_\phi = (\mathrm{P} - A).A^{-1}.k^{-1}.D_i.$$

Now, if we put $\eta = A^{-1}.k^{-1}$,

we finally find the following equations:

$$D_i = k.A. \begin{bmatrix} \mu_1 & 0 \\ 0 & \mu_2 \end{bmatrix},$$

$$D_\phi = (\mathrm{P} - A). \begin{bmatrix} \mu_1 & 0 \\ 0 & \mu_2 \end{bmatrix}.$$

Finally, the condition of attractiveness becomes

$$\mu_1. |S_1| + \mu_2. |S_2| > S^T.\tilde{\Phi}_r.$$

To complete the design of the observer, it now suffices to choose the correct observer parameters. The (p_1, p_2) parameters must be chosen to determine the dynamics of observer convergence and the (μ_1, μ_2) parameters to satisfy the conditions of attractiveness and stability for the observer.

5. Rotor speed MRAS observer

The rotor speed is estimated by using the MRAS (MRAS). This method consists of using 2 models. The first is the reference model, and the second is an adjustable model in which 2 components of the rotor flux, obtained from the measurements of the currents and stator voltages, are estimated.

The output of the reference model is compared with an adjustable observer-based model. The error is fed into an adaptation mechanism that is designed to assure the stability of the MRAS, as shown in Figure 3, which represents the observation technique structure.

By using the dynamic model of the asynchronous machine, formulated in a stator reference frame, (α, β), and by using measurements of the stator currents and voltages, we build 2 estimators of rotor flux.

5.1. Reference model

We can use the following voltage model as a reference model:

$$\begin{cases} \frac{d\Phi_{r\alpha}}{dt} = \frac{L_r}{L_m}. \left[v_{s\alpha} - R_s.i_{s\alpha} - \sigma L_s.\frac{di_{s\alpha}}{dt}\right] \\ \frac{d\Phi_{r\beta}}{dt} = \frac{L_r}{L_m}. \left[v_{s\beta} - R_s.i_{s\beta} - \sigma L_s.\frac{di_{s\beta}}{dt}\right] \end{cases} \tag{14}$$

However, in this work we have chosen to use the previous flux SMO as a reference model. This solution improves the MRAS performance and allows having a very low estimation error.

5.2. Adjustable model

Consider the last 2 equations of the induction machine model:

$$\begin{cases} \frac{d\Phi_{r\alpha}}{dt} = \lambda_r.(L_m.i_{s\alpha} - \Phi_{r\alpha}) - \omega.\Phi_{r\beta} \\ \frac{d\Phi_{r\beta}}{dt} = \lambda_r.(L_m.i_{s\beta} - \Phi_{r\beta}) + \omega.\Phi_{r\alpha} \end{cases} \tag{15}$$

We can see that Eq. (15) involves the ω parameter, so this estimator is considered an adjustable model.

By using the same input (stator voltage and stator current) in the 2 observer models, we define the error between the states of the 2 models below:

$$\begin{cases} \varepsilon_\alpha = \Phi_{r\alpha} - \hat{\Phi}_{r\alpha} \\ \varepsilon_\beta = \Phi_{r\beta} - \hat{\Phi}_{r\beta} \end{cases}.$$

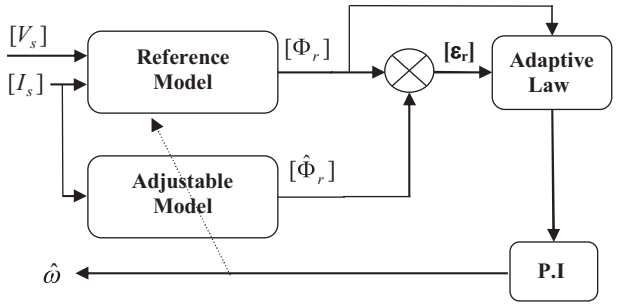

Figure 3. Rotor speed MRAS observer structure.

After deriving errors, we obtain the errors' dynamic equations as follows:

$$\begin{cases} \dot{\varepsilon}_\alpha = -\lambda_r.\varepsilon_\alpha - \omega.\Phi_{r\beta} + \hat{\omega}.\hat{\Phi}_{r\beta} \\ \dot{\varepsilon}_\beta = -\lambda_r.\varepsilon_\beta + \omega.\Phi_{r\alpha} - \hat{\omega}.\hat{\Phi}_{r\alpha} \end{cases} \tag{16}$$

By considering the following relation of speed estimation error:

$$\tilde{\omega} = \omega - \hat{\omega},$$

where $\hat{\omega}$ is the estimated speed, we can rewrite Eq. (16) as follows:

$$\begin{cases} \dot{\varepsilon}_\alpha = -\lambda_r.\varepsilon_\alpha - \tilde{\omega}.\Phi_{r\beta} - \hat{\omega}.\varepsilon_\beta \\ \dot{\varepsilon}_\beta = -\lambda_r.\varepsilon_\beta + \tilde{\omega}.\Phi_{r\alpha} + \hat{\omega}.\varepsilon_\alpha \end{cases} \tag{17}$$

In order to determine the observer's stability condition and then determine the adaptation mechanism that gives us the speed estimation, let us consider the following CLF:

$$V = \frac{1}{2}.\varepsilon_\alpha^2 + \frac{1}{2}.\varepsilon_\beta^2 + \frac{\tilde{\omega}^2}{2.\Gamma},$$

where Γ is a positive constant.

The CLF derivative is as below:

$$\dot{V} = \dot{\varepsilon}_\alpha.\varepsilon_\alpha + \dot{\varepsilon}_\beta.\varepsilon_\beta + \frac{\dot{\tilde{\omega}}.\tilde{\omega}}{\Gamma},$$

$$\dot{V} = -\lambda_r.\left(\varepsilon_\alpha^2 + \varepsilon_\beta^2\right) + \tilde{\omega}.\left[\frac{\dot{\tilde{\omega}}}{\Gamma} + \varepsilon_\beta.\Phi_{r\alpha} - \varepsilon_\alpha.\Phi_{r\beta}\right] \tag{18}$$

In order to make $\dot{V}$ negative definite, we can, for example, force the second term to be null, and then we can write:

$$\frac{\dot{\tilde{\omega}}}{\Gamma} + \varepsilon_\beta.\Phi_{r\alpha} - \varepsilon_\alpha.\Phi_{r\beta} = 0$$

$$\Rightarrow \dot{V} = -\frac{1}{T_r}.\left(\varepsilon_\alpha^2 + \varepsilon_\beta^2\right) < 0.$$

We have: $\dot{\tilde{\omega}} = -\dot{\hat{\omega}}$

$$\frac{\dot{\hat{\omega}}}{\Gamma} = \varepsilon_\beta.\Phi_{r\alpha} - \varepsilon_\alpha.\Phi_{r\beta}.$$

Thus, the corresponding adaptive law, which ensures the stability of the MRAS observer, is as follows:

$$\hat{\omega} = \Gamma \int (\varepsilon_\beta.\Phi_{r\alpha} - \varepsilon_\alpha.\Phi_{r\beta}).dt.$$

In order to decrease response time of estimation and ensure a null steady error, we use a PI controller as follows:

$$\hat{\omega} = k_p.\left(\varepsilon_\beta.\Phi_{r\alpha} - \varepsilon_\alpha.\Phi_{r\beta}\right) + k_i \int (\varepsilon_\beta.\Phi_{r\alpha} - \varepsilon_\alpha.\Phi_{r\beta}).dt,$$

where kp and ki are the proportional and integral positive.

The tracking performance of the speed estimation is dependent on these 2 adaptive gains. The integral gain ki is chosen high for fast tracking, and the proportional gain kp is chosen lower than ki to attenuate high-frequency signals. For more attenuation of noise, we associate a low-pass filter with a PI controller.

6. Load torque estimation

By considering that the load torque is constant or varies slowly with respect to speed and electrical parameters, we can reconstitute the load torque by using the estimated rotor flux and speed, as shown by the following expression:

$$\hat{T}_L = p\frac{L_m}{L_r}(\hat{\Phi}_{r\alpha}.i_{s\beta} - \hat{\Phi}_{r\beta}.i_{s\alpha}) - J.\frac{d\hat{\Omega}}{dt} - f.\hat{\Omega}.$$

7. Simulation results

Using MATLAB/Simulink, the proposed controller and observer techniques' performances have been verified by simulation results given in Figures 4–6 below. The parameters of the induction machine used in the simulation are given in the Table below.

Figure 4 shows us the simulation responses of the system for speed reference steps. In Figure 4a, the first step is given at 0 s from 0 to 100 rad/s, the second is from 100 rad/s to 150 rad/s at 0.8 s, and the last is down from 150 rad/s to 50 rad/s at 1.4 s. Figure 4a shows that the speed response is good, presenting a short response time of 0.28 s. The induction machine is loaded by 10 Nm at 0 s, as shown in Figure 4b. We can see in Figure 4b that the torque has good response and that the load torque estimation error is null. Figures 4b, 4c, and 4d respectively show that the currents, voltages, and torque respect the physical limits of the induction machine. Figure 4e shows that the decoupling between the torque and the flux is correct, and the flux and speed estimation errors are very low, as shown in Figures 4f, 4g, and 4h.

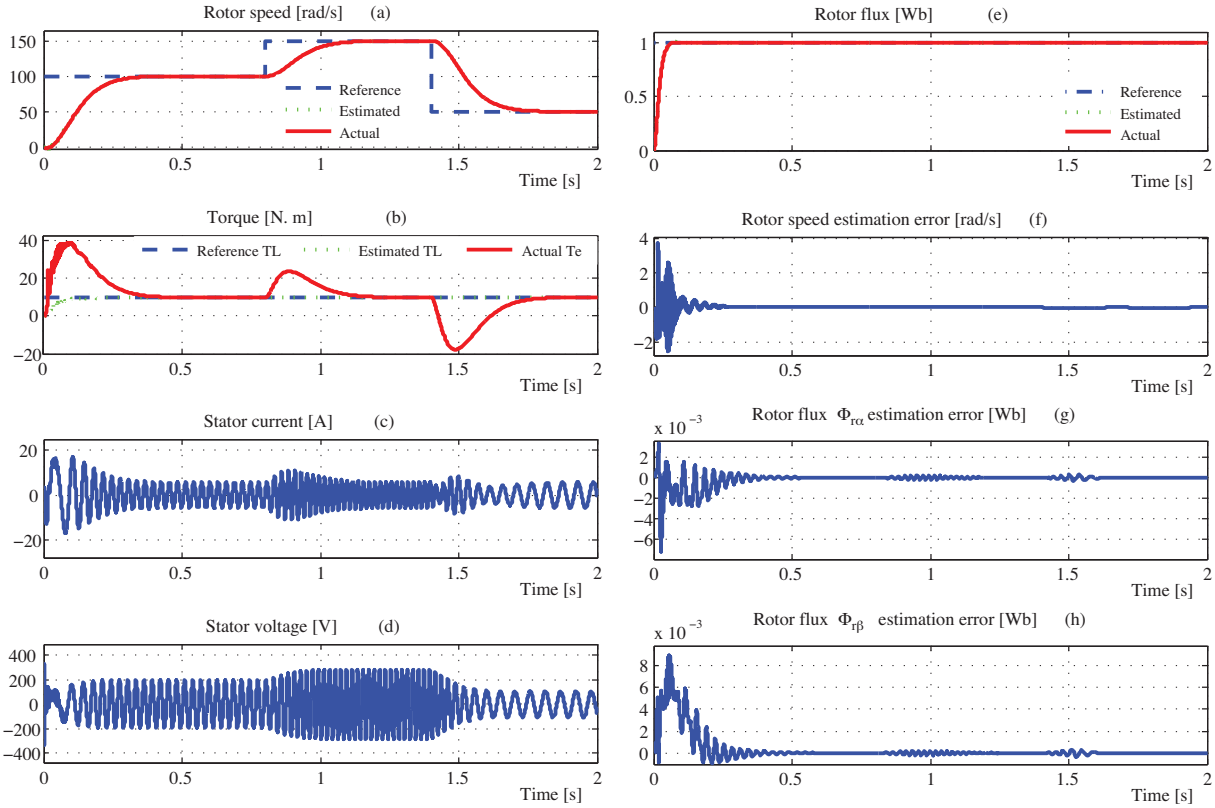

Figure 4. Simulation responses for steps of reference speed for 10 Nm in load torque.

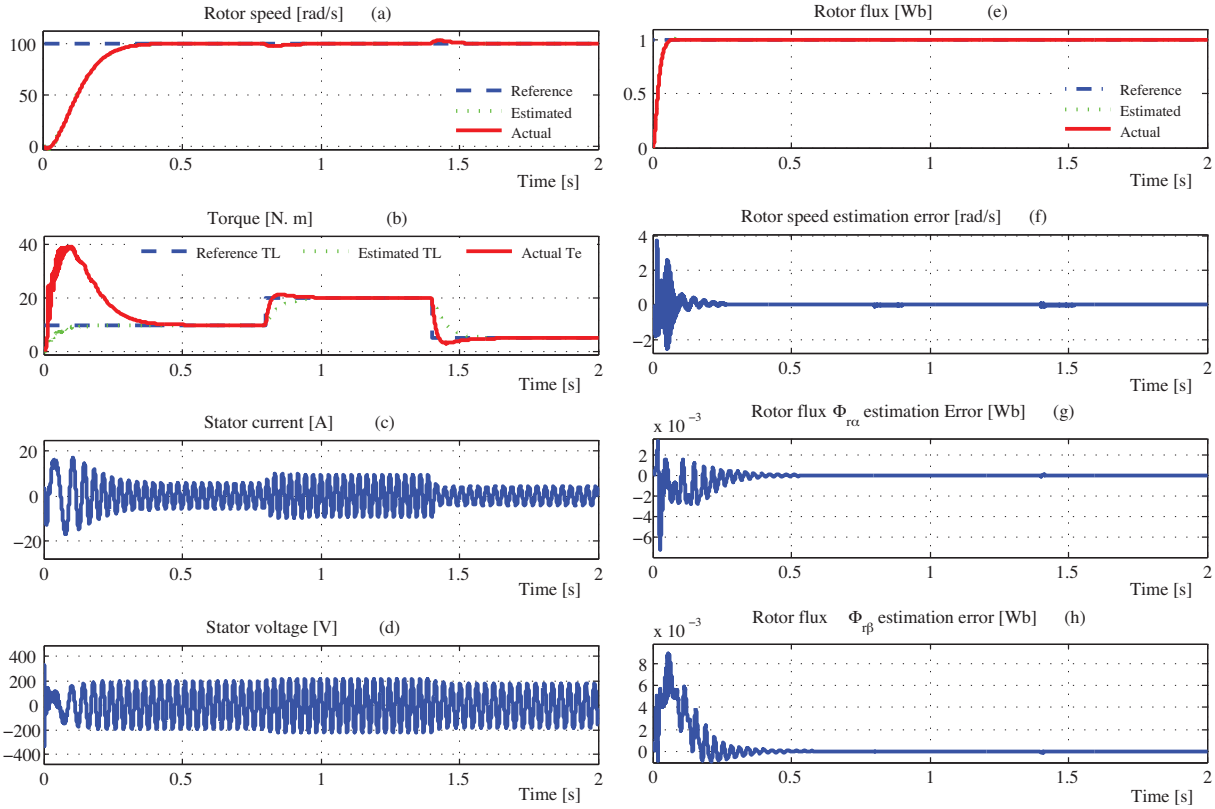

Figure 5. Simulation responses for steps of load torque at 100 rad/s in reference speed.

Figure 5 shows us the simulation responses of the asynchronous machine commanded for 100 rad/s of speed in Figure 5a, and for load torque steps in Figure 5b. The first step is given at 0 s from 0 to 10 Nm, the second is from 10 Nm to 20 Nm at 0.8 s, and the third is down from 20 Nm to 5 Nm at 1.4 s. We can observe in Figure 5b that the motor torque follows the load torque, and that the estimated load torque tracks its reference. Furthermore, we notice that stator currents and stator voltage are still under the maximum limits values of the induction machine, as shown in Figures 5c and 5d. Simulation results show that the speed and flux in Figure 5e are not influenced by torque variation. We can see in Figures 5f, 5g, and 5h that the estimation errors are very weak.

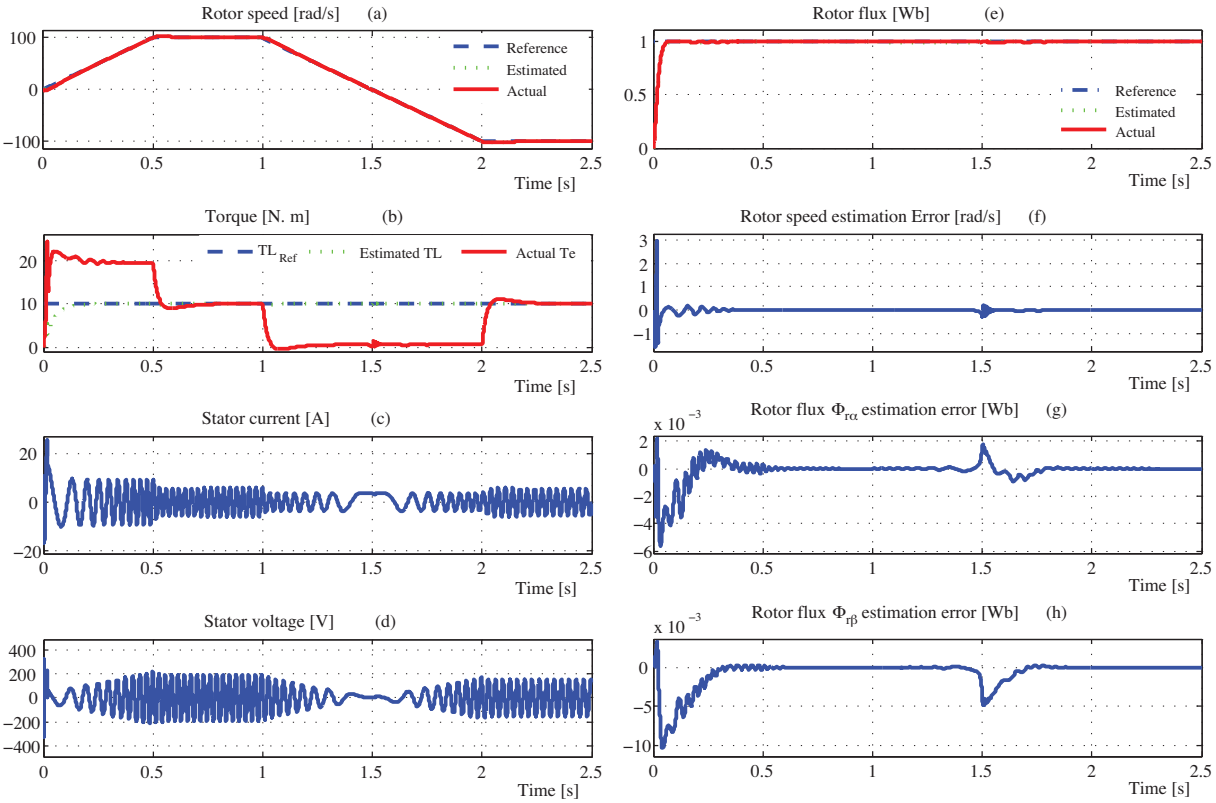

Figure 6. Simulation responses for ramps in reference speed and load torque = 10 Nm.

Figure 6 shows the simulation results in speed acceleration and deceleration mode with a load of 10 Nm. This proves that the controller (Figures 6a–6e) and the observer (Figures 6f–6h) maintain the same performance as the preceding simulations in terms of tracking trajectories, response time, and estimation errors.

8. Conclusion

In this article, we have performed a study of the sensorless speed control of an induction machine using the backstepping control technique associated with a speed observer based on the MRAS approach, governed by an adaptation law according to the flux's estimated errors. The estimation of the flux component was obtained by using a sliding mode observer. The simulation results show that this control and observation technique combination produces good performances and allows a complete decoupling between the flux and the torque. These performances are obtained with stator current, stator voltage, and torque, which respect the physical limits of the induction machine.

Table. The parameters of the induction machine.

Parameters		Values	Units
Power	P	3	kW
Voltage	U	380	V
Rated current	I	7.3	A
Rated speed	n	1440	rpm
Stator resistance	Rs	2.2	Ω
Rotor resistance	Rr	2.68	Ω
Mutual inductance	Lm	0.217	H
Stator inductance	Ls	0.229	H
Rotor inductance	Lr	0.229	H
Motor load inertia	J	0.047	kg m^2
Viscous friction coefficient	f	0.004	Ns/rad

Nomenclature

$\hat{x}, \tilde{x}$	Respectively the estimation and estimation error of x
$\dot{x}$ or $\frac{dx}{dt}$	Time derivative of x
$\Phi_r, \Phi_{r\alpha}, \Phi_{r\beta}$	Respectively the rotor flux and flux component in the stationary (α, β) axis
$i_{s\alpha}, i_{s\beta}$	Stator currents in the stationary (α, β) axis
$v_{s\alpha}, v_{s\beta}$	Stator voltages in the stationary (α, β) axis
R_r, R_s	Rotor and stator resistance
L_r, L_s, L_m	Respectively the rotor and stator cyclic inductances and the mutual cyclic inductance
Ω, T_L	Respectively rotor speed and load torque
J, f	Respectively rotor inertia moment and viscous friction coefficient

References

[1] F. Blaschke, "The principle of field orientation applied to the transvector closed-loop control system for rotating field machines", Siemens Review, Vol. 34, pp. 217–220, 1972.

[2] A. Mishra, P. Choudhary, "Speed control of an induction motor by using indirect vector control method", International Journal of Emerging Technology and Advanced Engineering, Vol. 2, Issue 12, pp. 144–150, 2012.

[3] A. Abbou, H. Mahmoudi, "Implementation of a sensorless speed control of induction motor using RFOC strategy", International Review of Electrical Engineering, Vol. 3, pp. 730–737, 2008.

[4] J. Ren, C.W. Li, D.Z. Zhao, "Linearizing control of induction motor based on networked control systems", International Journal of Automation and Computing, Vol. 6, pp 192–197, 2009.

[5] M. Moutchou, A. Abbou, H. Mahmoudi, M. Akherraz, "Sensorless input–output linearization speed control of induction machine", The International Workshop on Information Technologies and Communication, WOTIC'11, ID 123, 2011.

[6] M. Hajian, J. Soltani, G.R.A. Markadeh, S. Hosseinnia, "Input-output feedback linearization of sensorless IM drives with stator and rotor resistances estimation", Journal of Power Electronics, Vol. 9, No. 4, pp. 654–666, 2009.

[7] M.A. Duarte-Mermoud, J.C. Travieso-Torres, I.S. Pelissier, H.A. González, "Induction motor control based on adaptive passivity", Asian Journal of Control, Vol. 14, pp. 67–84, 2012.

[8] Z. Xu, J. Wang, P. Wang, "Passivity-based control of induction motor based on Euler-Lagrange (EL) model with flexible damping", International Conference on Electrical Machines and Systems, ICEMS 2008, pp. 48–52, 2008.

[9] V.I. Utkin, "Sliding mode control design principles and applications to electric drives", IEEE Transactions on Industrial Electronics, Vol. 40, pp. 23–36, 1993.

[10] E. Mukesh, K. Kumawat, J.V. Desai, "Speed control of induction motor using sliding mode controller", International Journal of Advancement in Electronics and Computer Engineering, Vol. 1, pp. 10–17, 2012.

[11] M.I. Galicia, A.G. Loukianov, J. Rivera, "Second order sliding mode sensorless torque regulator for induction motor", Decision and Control (CDC), 49th IEEE Conference, pp. 78–83, 2010.

[12] M.G. Aydeniz, İ. Şenol, "A Luenberger-sliding mode observer with rotor time constant parameter estimation in induction motor drives", Turkish Journal of Electrical Engineering & Computer Sciences, Vol. 19, pp. 901–912, 2011.

[13] R.A. Freeman, P.V. Kokotovic, "Backstepping design of robust controllers for a class of nonlinear systems", Proceedings of IFAC Nonlinear Control Systems Design Symposium, Bordeaux, France, pp. 307–312, 1992.

[14] M. Krstic, I. Kanellakopoulos, P. Kokotovic, Nonlinear and Adaptive Control Design, New York, Wiley, 1995.

[15] F. Ikhouane, M. Krstic, "Adaptive backstepping with parameter projection: robustness and asymptotic performance", Automatica, Vol. 34, pp. 429–435, 1998.

[16] R. Trabelsi, A. Kheder, M.F. Mimouni, F. M'sahli, "Backstepping control for an induction motor with an adaptive backstepping rotor flux observer", Control & Automation (MED), 2010 18th Mediterranean Conference, pp. 5–10, 2010.

[17] M. Moutchou, A. Abbou, H. Mahmoudi, "Sensorless speed backstepping control of induction machine, based on speed MRAS observer", International Conference on Multimedia Computing and Systems (ICMCS'12), IEEE Conference Publications, pp. 1019–1024, 2012.

[18] H.B. Imen, S. Hajji, A. Chaari, "Backstepping controller design using a high gain observer for induction motor", International Journal of Computer Applications, Vol. 23, pp. 1–6, 2011.

[19] D.V. Efimov, A.L. Fradkov, "Input-to-output stabilization of nonlinear systems via backstepping", International Journal of Robust and Nonlinear Control, Vol. 19, pp. 613–633, 2009.

[20] C.C. Peng, A.J. Hsue, C.L. Chen, "Variable structure based robust backstepping controller design for nonlinear systems", Nonlinear Dynamics, Vol. 63, pp. 253–262, 2011.

[21] F. Mehazzem, A. Ream, H. Benalla, "Sensorless nonlinear adaptive backstepping control of induction motor", ICGST-ACSE Journal, Vol. 8, pp. 1–8, 2009.

[22] C. Schauder, "Adaptive speed identification for vector control of induction motors without rotational transducers", IEEE Transactions on Industry Applications, Vol. 28, pp. 1054–1061, 1992.

[23] G. Tarchala, T.O. Kowalska, M. Dybkowski, "MRAS-type speed and flux estimator with additional adaptation mechanism for the induction motor drive", Transactions on Electrical Engineering, Vol. 1, pp. 7–12, 2012.

[24] M. Rashed, A.F. Stronach, "A stable back-EMF MRAS-based sensorless low speed induction motor drive insensitive to stator resistance variation", IEE Proceedings Electric Power Applications, Vol. 151, pp. 685–693, 2004.

[25] K.K. Prajapat, V.N. Lal, S. Shuchi, R.K. Srivastava, "Speed sensorless vector control of induction machine based on the MRAS theory", Journal of Electronic and Electrical Engineering, Vol. 2, pp. 30–36, 2011.